

FIG. 3. Delay of the peak pulse versus input energy (a) obtained with P_{14} pulses, and (b) calculated for a nondegenerate (solid line) and a highly degenerate (broken line) transition (Q_{10}).

lines are reduced. We feel that in our case (P_{12} and P_{14} frequencies) no overlap of the SF_6 tran-

sitions occurs even at 300°K .

The authors are very grateful to Professor W. Kaiser for numerous valuable discussions. They also thank Dr. F. Keilmann, Institut für Plasmaphysik, Garching, for making available to us two Ge:Hg detectors.

- ¹C. K. N. Patel and R. E. Slusher, *Phys. Rev. Lett.* **19**, 1019 (1967); C. K. N. Patel, *Phys. Rev. A* **1**, 979 (1970).
- ²C. K. Rhodes and A. Szöke, *Phys. Rev.* **184**, 25 (1969).
- ³F. A. Hopf and M. O. Scully, *Phys. Rev. B* **1**, 50 (1970).
- ⁴S. L. McCall and E. L. Hahn, *Phys. Rev.* **183**, 457 (1969); F. A. Hopf and M. O. Scully, *Phys. Rev.* **179**, 399 (1969).
- ⁵J. P. Gordon, C. H. Wang, C. K. N. Patel, R. E. Slusher, and W. J. Tomlinson, *Phys. Rev.* **179**, 294 (1969).
- ⁶H. M. Gibbs and R. E. Slusher, *Phys. Rev. Lett.* **24**, 638 (1970).
- ⁷C. K. Rhodes, A. Szöke, and A. Javan, *Phys. Rev. Lett.* **21**, 1151 (1968); F. A. Hopf, C. K. Rhodes, and A. Szöke, *Phys. Rev. B* **1**, 2833 (1970).
- ⁸M. W. Goldberg and R. Yusek, *Appl. Phys. Lett.* **17**, 349 (1970).
- ⁹C. L. Tang and H. Statz, *Appl. Phys. Lett.* **10**, 145 (1967).
- ¹⁰R. P. Feynman, F. L. Vernon, and R. W. Hellwarth, *J. Appl. Phys.* **28**, 49 (1957).
- ¹¹C. K. N. Patel and R. E. Slusher, *Phys. Rev. Lett.* **20**, 1087 (1968); P. Rabinowitz, R. Keller, and J. T. LaTourette, *Appl. Phys. Lett.* **14**, 377 (1969).
- ¹²G. B. Hocker and C. L. Tang, *Phys. Rev.* **184**, 356 (1969).

Differential Cross Sections for K -Shell Ionization of Surface Atoms by Electron Impact*

Robert L. Gerlach and A. R. DuCharme
Sandia Laboratories, Albuquerque, New Mexico 87115
 (Received 6 May 1971)

We report first differential cross-section measurements for inner-shell ionization of surface atoms by electron impact. Comparison is made with calculations derived from a simple extension of the Burhop theory for ionization of isolated atoms. The trends of the predicted values are in qualitative agreement with experiment.

Excitation or ionization of the inner shells of atoms in molecular gases and in solids by electron impact has received considerable attention.¹⁻³ A related phenomenon is the ionization of atoms adsorbed on solid surfaces. Measurements of total inner-shell ionization cross sections as a function of primary energy have been made for gas, solid, and surface systems.¹⁻⁴ Until now,

however, differential cross sections, which provide a better test of inelastic scattering theory, have been lacking. This has been due partially to sensitivity and absorption problems involved in the measurements. Detection of the ionization of chemisorbed atoms on surfaces has the distinct advantage that large numbers of atoms ($\sim 10^{13}$) are involved in the scattering, resulting

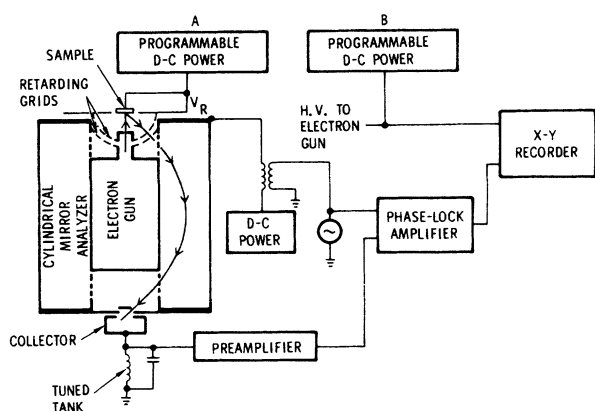


FIG. 1. Simplified schematic of apparatus used for differential cross-section measurements. Loss spectra are obtained with power supply *A* fixed, *B* programmed, and with second-harmonic detection of the energy-analyzed current.

in large signals. In addition, absorption of the primary beam is not important since a single layer of atoms is examined.

A technique, ionization spectroscopy, was recently developed by one of us for the identification of surface atoms from their electron binding energies.⁵ In ionization spectroscopy, inelastically backscattered electrons are detected which have suffered collisions with bound atomic electrons. As a result of the interaction, core electrons are ejected to unfilled states above the Fermi level defined by the substrate. The energy and angle of the scattered electrons are confined to narrow limits, facilitating the measurements of differential cross sections for inner-shell ionization of surface atoms.

The apparatus for differential ionization cross-section observation is shown in Fig. 1. The secondary electrons are energy analyzed by the two-stage, retarding-potential, cylindrical mirror analyzer. Electrons which have been scattered between 128° and 148° from the incident beam direction are detected with an energy spread of 2 eV. Separation of characteristic loss features from fixed energy peaks in the secondary-electron energy distribution is accomplished by sweeping the electron-gun potential while maintaining fixed dc voltages to the analyzer cylinder and sample. The second derivative of the secondary-electron energy distribution with respect to secondary-electron energy, $\partial^2 N(E, E_p) / \partial E^2$, as a function of primary energy E_p is obtained by standard synchronous detection techniques in order to suppress the background with respect to the sharp ionization features.

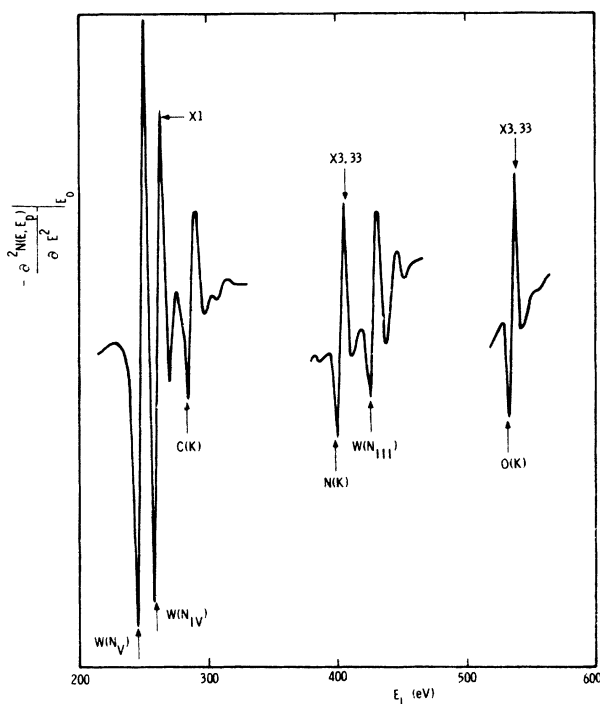


FIG. 2. Loss spectra for C, N, and O adsorbed independently on W. Tabulated electron binding energies (Ref. 6) are indicated by arrows. The analyzer band-pass energy E_0 used for each curve is such that the reduced primary energy $X = E_p / E_i = 2.0$ for the C, N, and O peaks, where E_p is the primary energy and E_i is the ionization energy. Loss energy E_L is measured with respect to the low energy minimum of the elastic peak (Ref. 5).

Typical energy-loss spectra for carbon (ethylene), nitrogen, and oxygen adsorbed on W (100) are shown in Fig. 2. The double differentiated features have intensity proportional to the sudden ionization current arising as the loss energy becomes sufficient for ejection of *K*-shell electrons to the Fermi level. By comparing the intensities of these peaks with the elastic peak of known current, absolute differential ionization cross sections may be computed if the density of adsorbed atoms is known. Uncertainties in the atom density and in corrections made for the shapes and widths of the ionization peaks lead to experimental uncertainties of about a factor of 3 in the absolute cross sections so determined.

Differential *K*-shell cross sections as a function of reduced primary energy are shown in Fig. 3. The differential cross sections decrease monotonically with primary energy shortly after threshold energy is reached. This rapid decrease in cross section illustrates the fact that large changes in momentum between incident and scattered electrons are unfavorable.

The Burhop⁷ first Born approximation theory for ionization by electron impact has been moderately successful in describing the total cross sections for *K*-shell ionization of Ni, Ag, and Hg. The theory has not been tested for low-energy, inner-core *K*-shell ionizations or by differential cross section measurements. Such a situation arises here, but with the complication that the atoms are adsorbed on a solid surface. We adapt the Burhop theory to surface atoms by placing the zero of the kinetic-energy scale at the bottom of the conduction band for the tungsten substrate. This assumes that the potential wall between adatom and surface is near the bottom of the conduction band.

The Burhop theory uses a plane wave to represent the incident electron and a spherical wave for the scattered electron. A hydrogenic wave function and a Coulomb wave function represent the initial and final states of the *K*-shell electron. The following expression is found for the differential cross section⁷:

$$I(K, \kappa) dK d\kappa = \frac{2^{11} \pi \mu^6 \kappa [K^2 + \frac{1}{3}(\mu^2 + \kappa^2)] [\mu^4 + 2\mu^2(K^2 + \kappa^2) + (K^2 - \kappa^2)^2]^{-3}}{a_0^2 k^2 K [1 - \exp(-2\pi\mu/\kappa)]} \times \exp\left[\frac{-2\mu}{\kappa} \arctan \frac{2\mu\kappa}{K^2 - \kappa^2 + \mu^2}\right] dK d\kappa, \quad (1)$$

where $\mu = Z/a_0$ with a_0 the Bohr radius.⁸ The initial and final momenta of the incident electron, k and k' , are related to the momentum of the ejected electron κ and the ionization energy E_i via the energy relation

$$(\hbar^2/2m)(k^2 - k'^2) = E_i + \hbar^2 \kappa^2/2m. \quad (2)$$

For the purpose of comparing with experimental data we used the momentum-transfer definition to obtain the angular dependence:

$$K = |\vec{k} - \vec{k}'| = (k^2 + k'^2 - 2kk' \cos\theta)^{1/2}. \quad (3)$$

We made the final state of the ejected electron compatible with the metal-surface environment and the experimental conditions by restricting the energy to a small region (2 eV) above the Fermi level of W.

Calculated differential cross sections for inner-shell ionization of surface atoms are shown in Fig. 3 where they are compared with the experimental results. The theory predicts the general shape dependence found experimentally for differential cross section versus reduced primary energy. In addition, the experimental trend of increased differential cross section with decreased atomic number is in agreement with our calculations. For reduced energies less than 2, the theory underestimates the experimental values for all three elements studied, but disagree-

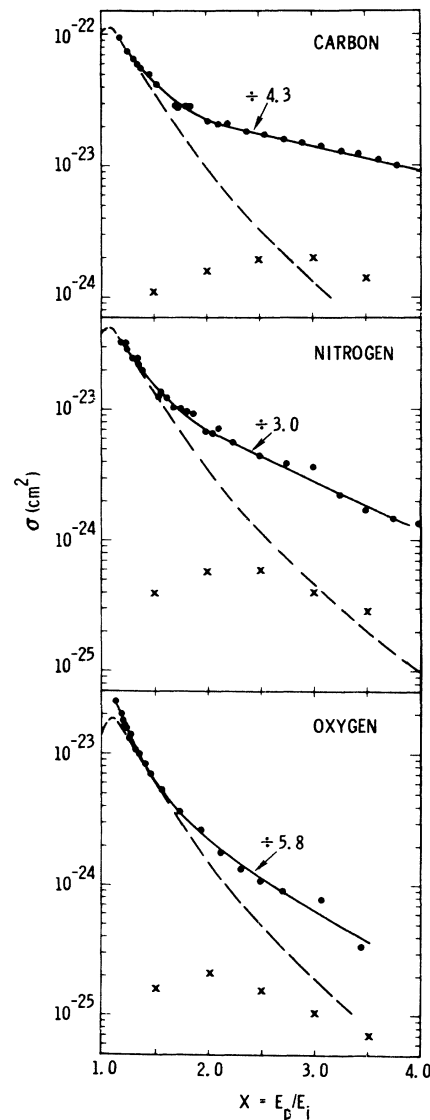


FIG. 3. Differential cross sections for *K*-shell ionization of C, N, and O adsorbed on W (100). The experimental differential cross sections (solid lines) are reduced as specified to be tangent to the theoretical curves (dashed lines). The points indicated by x's denote estimated cross sections for double scattering.

ment is never more than an order of magnitude. For reduced energies greater than 2, the disagreement is more extreme.

Double scattering must be considered as a possible explanation for the differences between experiment and the Burhop theory. The inelastic ionization scattering is sharply peaked in the forward direction, whereas the elastic scattering factor for W is rather smooth for large angles. Therefore, a forward ionization event followed by backward elastic scattering by the W substrate and vice versa are the dominant double-scattering terms. The double-scattering cross section σ_{ds} may be estimated from the equation

$$\sigma_{ds}(X) = \sigma_{fs}(X)R(X) + R(X-1)\sigma_{fs}(X), \quad (4)$$

where X is the reduced primary energy, σ_{fs} is the cross section for forward ionization scattering, and R is the observed elastic reflection coefficient for electrons scattered into the 20° -wide analyzer sperture. The elastic reflection coefficient ranges from about 10^{-3} to 10^{-4} for primary energies from 100 to 1500 eV. The forward ionization scattering cross section was calculated for angles within 20° of the forward direction where more than half of the scattering occurs. The double scattering estimated from Eq. (4) is shown by x's in Fig. 3 and indicates that single scattering dominates for reduced energies up to at least 2.5. Thus it is unlikely that double scattering can account for the major differences between experiment and the single-event inelastic

theory for backscattering.

Although the Burhop theory involves many approximations, it does provide qualitative agreement with these experiments. We are currently extending our studies to include other elements. We are especially interested in species whose surface coverages may be more precisely determined. It is hoped that more precise measurements of differential cross sections for inner-shell ionization will allow assessment of the various approximations involved in the present model.

*Work supported by the U. S. Atomic Energy Commission.

¹M. R. H. Rudge, Rev. Mod. Phys. **40**, 546 (1968).

²M. J. Van Der Wiel, Th. M. El-Sherbini, and C. E. Brion, Chem. Phys. Lett. **7**, 161 (1970).

³Y. K. Kim and M. Inokuti, Phys. Rev. A **3**, 665 (1971).

⁴H. E. Bishop and J. C. Riviere, Surface Sci. **24**, 1 (1971).

⁵R. L. Gerlach and D. W. Tipping, Rev. Sci. Instrum. **42**, 151 (1971).

⁶K. Siegbahn *et al.*, ESCA—Atomic Molecular and Solid State Structures by Means of Electron Spectroscopy (Almqvist and Wiksells Boktryckeri AB, Uppsala, Sweden, 1967).

⁷E. H. S. Burhop, Proc. Cambridge Phil. Soc. **36**, 43 (1940).

⁸The term $\frac{1}{2}(u^2 + \kappa^2)$ was corrected to $\frac{1}{3}(u^2 + \kappa^2)$ by A. M. Arthurs and B. L. Moiseiwitsch, Proc. Roy. Soc., Ser. A **247**, 550 (1958).

Experimental Atomic-Electron Binding Energies in Fermium

F. T. Porter and M. S. Freedman

Chemistry Division, Argonne National Laboratory, Argonne, Illinois 60439

(Received 15 June 1971)

Atomic electron binding energies for ${}_{100}\text{Fm}$ have been measured ($\pm \sim 10$ eV) for shells K , L_{1-3} , N_{1-5} , $N_{6,7}$, O_{1-3} , $O_{4,5}$, and $P_{2,3}$ from conversion electron spectroscopy in the β decay ${}^{254}\text{mEs} \rightarrow {}^{254}\text{Fm}$. The $P_{2,3}$ value of 24 ± 9 eV is unexpectedly low compared to empirical and to self-consistent field-based extrapolations. Preferential judgements among published actinide binding-energy tabulations are presented.

Because of the current activity in electron and x-ray spectroscopy in transplutonic elements (and even for specifically chemical and optical spectroscopic interest), and to facilitate precise extrapolation of atomic properties beyond the known species, we present experimental electron binding energies (K through P shells) for

fermium. These values are obtained solely via precision spectroscopy of internal conversion electrons. Similar but less precise measurements have been made for $Z=97$ ¹ and $Z=98$.² Recent binding-energy determinations³ at $Z=96$ used transition-energy and conversion-line energy measurements.